JOURNAL OF MATERIALS SCIENCE 14 (1979) 354–364

Carbide precipitation in certain alloys of the Co-Ni-Cr-C system

P. A. BEAVEN
Department of Metallurgy and Science of Materials, University of Oxford, UK

P. R. SWANN
GATAN Incorporated, Pittsburgh, Pennsylvania USA

D. R. F. WEST
Department of Metallurgy and Materials Science, Imperial College, London, UK

An investigation is reported of structural and hardness changes during the precipitation of $Cr_{23}C_6$ from f c c supersaturated solid solution in various alloys of the Co–Ni–Cr–C system containing 25 wt % Cr and 0.15 to 0.25 wt % C. The work extends results previously reported on a Co–25.3 wt % Cr–0.26 wt % C alloy, by studying the effect of adding nickel to replace cobalt (either wholly or completely) and hence changing the stacking fault energy. The addition of 10% nickel was found to increase the nucleation rate of matrix precipitation; precipitate particles also nucleated on partial dislocations with associated stacking fault formation. With approximately 55% nickel and 0.15% carbon, there was little matrix precipitation; instead precipitation occurred predominantly on dislocations, as rods growing along ⟨1 1 0⟩ directions; the main climb morphology was the formation of dislocation dipoles. Substantial precipitation hardening effects were obtained, particularly in the cobalt-rich alloys with 0.25% carbon. In a ternary Ni–25 wt % Cr–0.25 wt % C alloy, a non-uniform precipitate dispersion formed involving nucleation in the matrix and on dislocations. An investigation was also made of the effect of prior strain (1 to 10%) on the ageing of the Co–25.3 wt % Cr–0.26 wt % C alloy. Deformation of the f c c solution-treated material produced faulting and also the formation of h c p ϵ phase. On ageing, $Cr_{23}C_6$ precipitation occurred within the ϵ lamellae; at long ageing times after 10% deformation carbide particle coarsening, and matrix recrystallization occurred concurrently, and the recrystallization was accompanied by the transformation of the f c c matrix to h c p ϵ phase.

1. Introduction

In commercial cobalt-based superalloys, carbide dispersions contribute substantially to high temperature strength, and alloys are typically based on the Co–Cr–C system. Investigations reported on such superalloys, although less extensive than those on austenitic steels, have elucidated some of the structural aspects of carbide precipitation, e.g. [1–5]. In the case of typical nickel-based superalloys, the high temperature strength depends to a large extent on γ' dispersions; however, the carbide precipitation at grain boundaries is of importance in relation to creep properties and it is also of interest to study the potentialities of intra-granular precipitation as a strengthening mechanism.

The work reported here is concerned with the precipitation of $Cr_{23}C_6$ in certain alloys of the Co–Ni–Cr–C system. The work develops from previously reported results of $Cr_{23}C_6$ precipitation from supersaturated solid solution in a Co–25.3 wt % Cr–0.26 wt % C alloy [3–5]. The

© 1979 Chapman and Hall Ltd. Printed in Great Britain.

effect is reported of adding nickel to replace cobalt, the highest nickel content studied being a ternary composition Ni–25 wt % Cr–0.25 wt % C. This range of compositions selected was intended to allow a study of the influence of matrix stacking fault energy on the precipitation processes. An investigation has also been made of the effect of prior plastic strain on the ageing of the Co–25.3 wt % Cr–0.26 wt % C alloy.

TABLE I Alloy compositions (wt %)

Alloy	Co	Ni	Cr	C
1	balance (74.44)	–	25.3	0.26
2	balance (64.75)	10	25	0.25
3	balance (64.85)	10	25	0.15
4	20	balance (54.85)	25	0.15
5	–	balance (74.75)	25	0.25

2. Experimental procedure

The alloy compositions are listed in Table I. The Co–25.3 Cr–0.26 C alloy, previously studied by Ramaswamy *et al.* [3] was prepared by C.N.R.M. Belgium, and was supplied in wrought form. This was taken as a basis of comparison for studying the effect of an addition of 10 wt % nickel (alloy 2). The effect of reducing the carbon content to 0.15 wt % was studied in a nickel-containing alloy (3). The nickel-based alloy, (5) (Ni–25 Cr–0.25 C) was chosen for comparison with the cobalt-based composition, but constitutional data are lacking for the Ni–Cr–C system and it was found that the carbon content chosen was considerably in excess of the solubility limit. Accordingly, in choosing a nickel-based alloy containing cobalt, a carbon level of 0.15% was selected (alloy 4), providing a comparison with alloy 3.

Alloys 2 to 5 were prepared as arc-melted ingots (~50 g) and the procedure involved several remelts to achieve homogeneity. To minimize loss of carbon during arc-melting the carbon levels were controlled by using the Co–Cr–C alloy and binary Co–2.4 wt % C and Ni–1.7 wt % C alloys as master alloys. The purities of the basis materials used in the preparation of the binary master alloys and in making up furnace charges were nickel (~99.95%), cobalt (99.9% minimum) and chromium (~99.8%). Except for the Co–Cr–C alloys, chemical analysis was not carried out. However, by using the master alloys, and with only a small weight loss occurring in melting, the actual compositions are considered to be close to the values listed in Table I.

The arc melted ingots were sealed in silica capsules under 1/3 of an atmosphere of high purity argon, and were homogenized for 24 h at 1300° C followed by water quenching. The ingots were then hot-rolled at 1200° C to sheet of thickness ~0.7 to 1.0 mm. After surface grinding of the sheet, samples were cut for structural and hardness studies; these samples were sealed in silica capsules under 1/3 of an atmosphere of argon and solution treated for 1 h at 1300° C. The usual water quenching procedure involved breaking the capsules below the surface of the water bath. For ageing treatments carried out in the range 650 to 1100° C, specimens were again sealed in silica capsules under argon. Some specimens were strained at room temperature (1% in tension, or 5 or 10% by rolling) prior to ageing.

The preparation of specimens for light microscopical examination involved electrolytic etching using 5% aqua regia or 10% HCl in ethanol. Specimens for electron microscopy were prepared by electropolishing disc specimens (~0.01 mm thick) using a jetting technique with 20% perchloric acid/80% acetic solution at ~15° C. In some cases, discs were given a final polish using the window technique and a more dilute electrolyte.

3. Experimental results

3.1. Structural features of solution-treated materials

The matrix structure of all the alloys after solution treatment and water quenching was f c c, but some carbide particles remained undissolved; the amount of carbide was appreciably greater in the nickel-based alloys. The grain size was typically about 0.1 mm.

In the cobalt-based alloys the dislocation substructure was inhomogeneous; in some regions dislocations were widely dissociated but in others they were undissociated. Clusters of overlapping stacking faults (found to be intrinsic) were a common feature [5]. The density of faults was related primarily to the distribution and amount of undissolved carbides, and a high density of faults existed around the carbide particles.

In the nickel-based alloys the dislocations lay in planar arrays, and no dissociation was observed. Perfect dislocations were "punched out" around carbide particles. In the Ni–Cr–C alloy (5) there was evidence of localized melting having occurred at the grain boundaries during solution treatment.

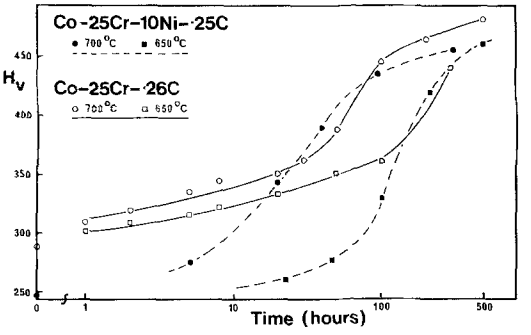

Figure 1 Hardness versus ageing time data for the Co–25 Cr–0.26 C and the Co–25 Cr–10 Ni–0.25 C alloys.

3.2. Carbide precipitation in the Co–25 Cr–10 Ni–C alloys

The hardness response on ageing the Co–25 Cr–10 Ni–0.25 C alloy is shown in Fig. 1, and also in Table II, together with data for the other alloys. The hardness increments were slightly greater in the Co–25 Cr–10 Ni–0.25 C alloy than in the Co–25.3 Cr–0.26 C alloy for comparable heat treatments, although the levels of hardness achieved at long ageing times were slightly lower. In the Co–25 Cr–10 Ni–0.15 C alloy the increments were substantially smaller than in the higher carbon material.

Electron microscopical examination of the 0.25 C alloy aged for 2 h at 700° C showed a structure similar to that of the ternary alloy as previously reported [5]; matrix nucleated particles of $Cr_{23}C_6$ of ~80 Å diameter were present with a greater particle density than in the ternary alloy (Fig. 2). Repeated nucleation of carbide also occurred on the Frank partials bounding extrinsic stacking faults developed from matrix carbide particles and the fault density was significantly greater than in the ternary alloy; the faults formed at shorter ageing times. Dislocation climb precipitation was more widespread than in the ternary alloys; it occurred on {1 1 0} planes, and was frequently initiated by matrix particles, in a similar manner to the nucleation of stacking faults.

TABLE II Hardeness increments obtained on ageing at 700° C

Alloy	Solution treated hardness (H_V)	Increment (H_V)	Ageing time (h).
1 Co–25.3 Cr–0.26 C	290	185	500
2 Co–25 Cr–10 Ni–0.25 C	250	210	300
3 Co–25 Cr–10 Ni–0 15 C	215	65	200
4 Ni–25 Cr–20 Co–0.15 C	165	105	50

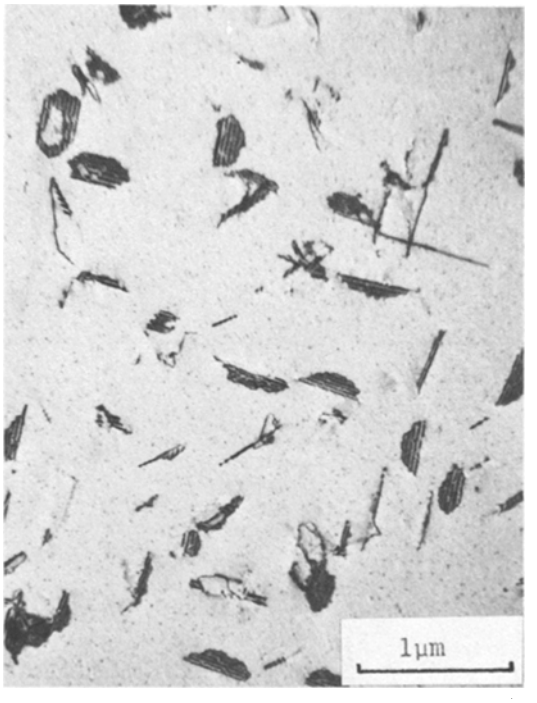

Figure 2 Co–25 Cr–10 Ni–0.25 C alloy, solution treated 1 h at 1300° C, water quenched and aged 2 h at 700° C. Bright-field micrograph showing the matrix precipitates and stacking faults.

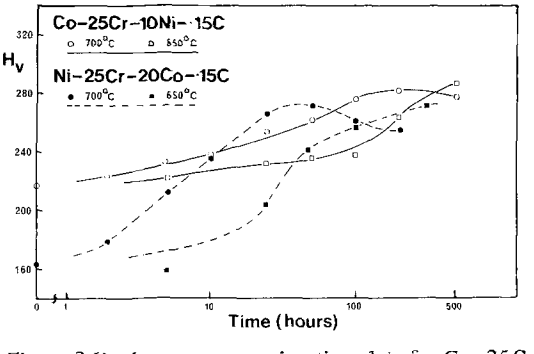

Figure 3 Hardness versus ageing time data for Co–25 Cr–10 Ni–0.15 C and Ni–25 Cr–10 Ni–0.15 C alloys.

Examination of the lower carbon alloy (0.15 C) aged for 24 h at 650° C showed the presence of extensive matrix precipitation comparable in amount with the ternary alloy. In the later stages of ageing the particles coarsened more rapidly than in the 0.25 C alloy.

3.3. Carbide precipitation in the Ni–25 Cr–20 Co–0.15 C alloy

The hardness versus ageing time curves in Fig. 3 and the data in Table II show that the hardness increments were greater in the Ni–25 Cr–20 Co–

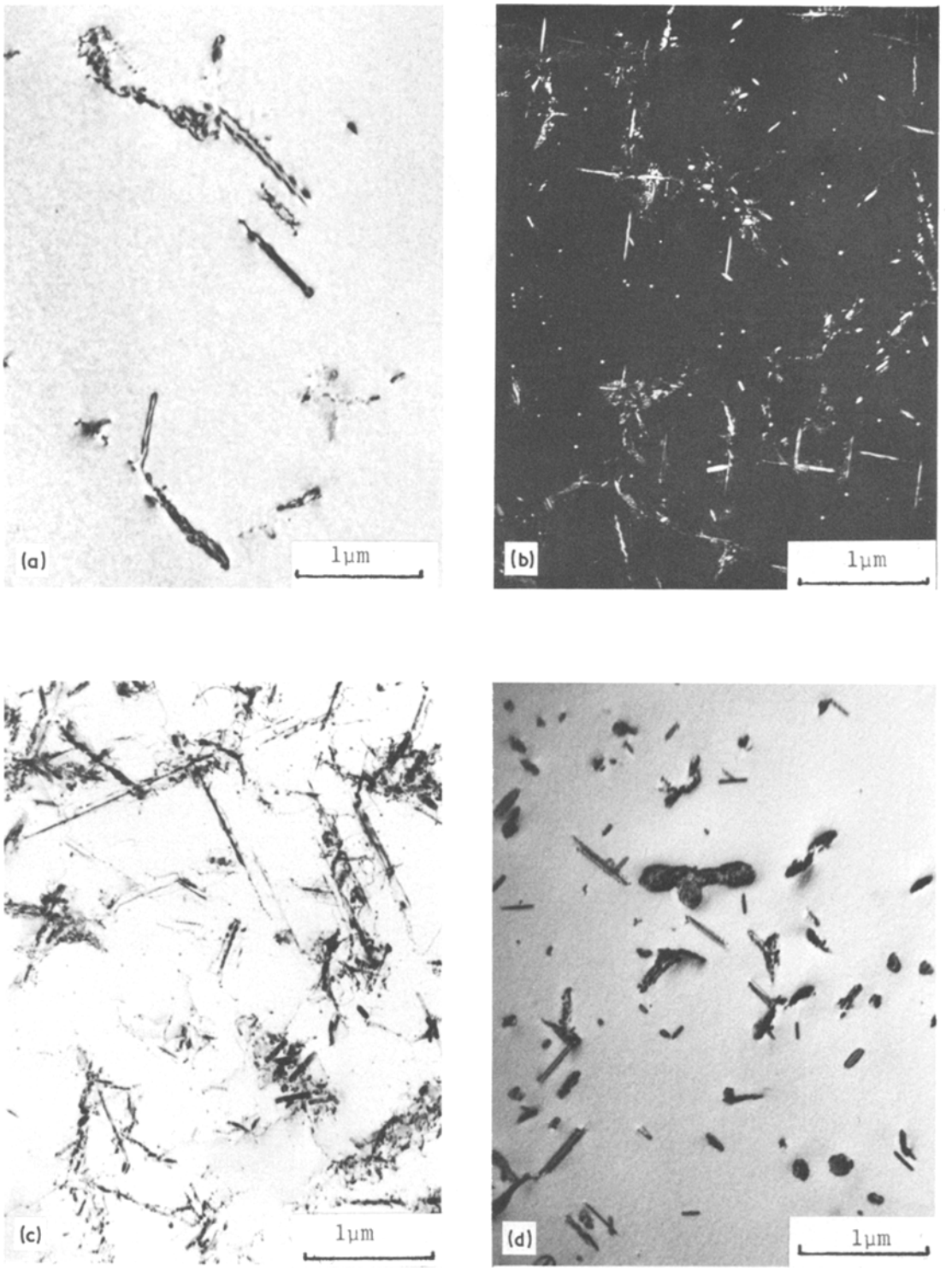

Figure 4 Ni–25Cr–20Co–0.15C alloy solution treated 1 h at 1300° C and water quenched. (a) Aged 1 h at 700° C. Bright-field micrograph showing dislocation dipoles and thin rods of $Cr_{23}C_6$. (b) Aged 24 h at 650° C. Dark-field micrograph showing matrix-nucleated particles and dislocation-nucleated rods. (c) Aged 100 h at 650° C. Bright-field micrograph showing complex tangles of dislocation and particles. (d) Aged 80 h at 600° C. Bright field micrograph showing growth of matrix particles along ⟨1 1 0⟩ directions.

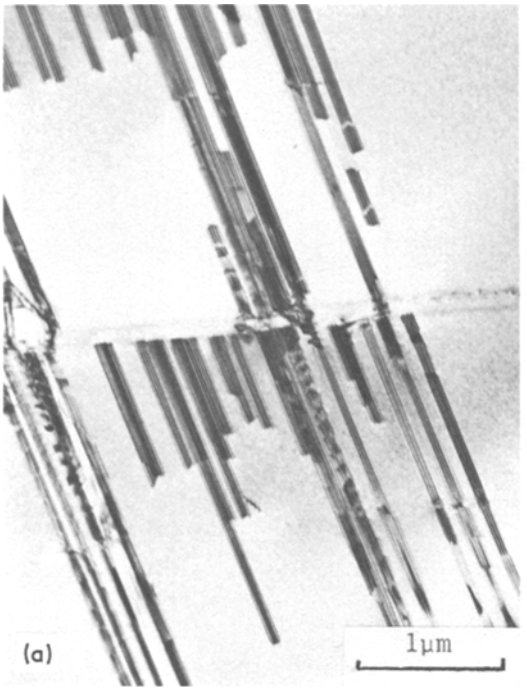

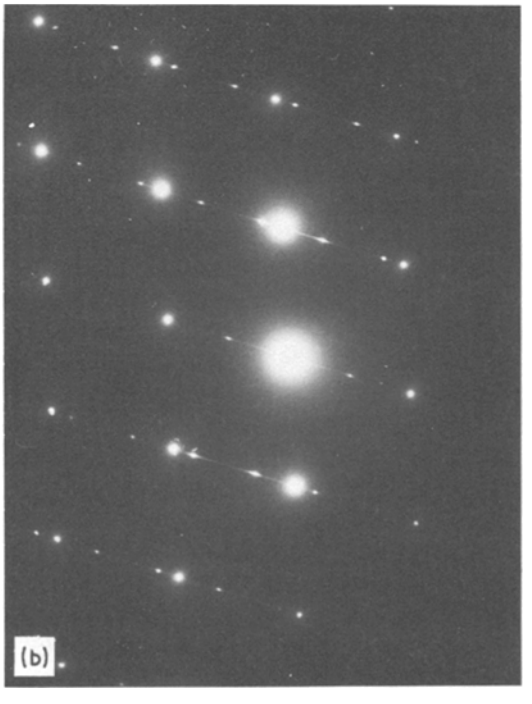

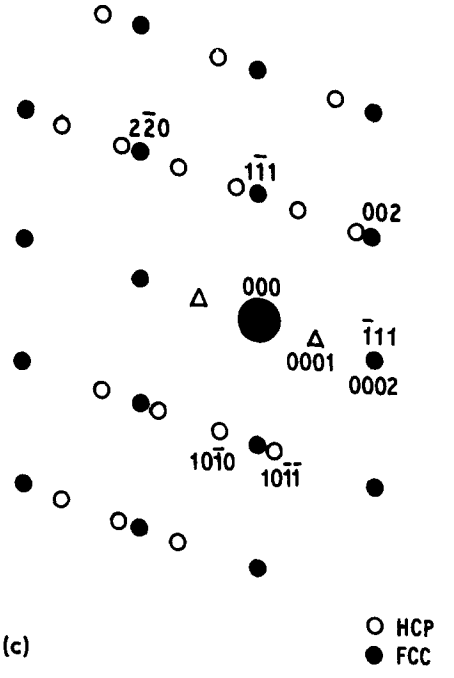

Figure 5 Co–25Cr–0.26C alloy solution treated 1 h at 1300° C and water quenched; deformed 1%. (a) Bright-field micrograph showing thin ϵ lamellae of h c p ϵ phase. (b) Diffraction pattern showing presence of h c p ϵ phase, with streaked reflections associated with thin ϵ lamellae. (c) Diagram identifying reflections in (b).

0.15 C alloy than in the Co–25 Cr–10 Ni–0.15 C alloy. There was little variation of the increment with change in ageing temperature.

After 1 h at 700° C (Fig. 4a) carbide nucleation had occurred predominantly on dislocations, only a few matrix precipitates being observed. Some repeated nucleation in association with dislocation climb was apparent, but the predominant climb morphology was the formation of dislocation dipoles. This occurred by the climb of short segments of the original dislocations, and was associated with the formation of thin rods of $Cr_{23}C_6$ along ⟨1 1 0⟩ directions. Selected area diffraction examination confirmed the presence of $Cr_{23}C_6$ exhibiting the cube–cube orientation relationship.

The structure after ageing for 24 h at 650° C (Fig. 4b) showed the following features: (i) there was a low density of matrix-nucleated particles ($\sim 10^{13}$ cm^{-3}), of diameter 170 Å. (ii) Dislocation-nucleated rods were present of thickness ~150 to 200 Å, and length up to 0.5 μm. Growth of these rods was rapid, along ⟨1 1 0⟩ directions, and the dislocation remained attached to the tip of the rod, producing the observed dipole. (iii) Repeated nucleation subsequently occurred on the dipoles as they climbed on planes whose normals were perpendicular to the growth direction of the rod; this growth took place on {1 1 0} planes, and also appeared to occur on {1 1 1} planes on some occasions. (iv) In some cases climb occurred more uniformly on {1 1 0} planes normal to the Burgers

vectors producing arrays of carbides ~80 Å in diameter on {1 1 0} planes. This behaviour was associated with dislocations of pure edge character, and rod formation was usually associated with dislocations of mixed or screw character. (v) Commonly, complex tangles of dislocations and particles were produced at long ageing times (Fig. 4c).

Ageing at 600° C proceeded less rapidly, and Fig. 4d shows the microstructure after 80 h ageing. Similar climb mechanisms were operative, but matrix nucleation was more widespread. The matrix particles grew rapidly along ⟨1 1 0⟩ directions, producing elongated loops similar to the dipoles observed at 650 and 700° C. Repeated nucleation was also more extensive.

3.4. Carbide precipitation in the Ni–25 Cr–0.25 C alloy

Electron microscopical examination of specimens aged for 5 h at 700° C revealed the precipitate distribution to be inhomogeneous and to be influenced by the presence of the high density of undissolved carbide particles. These undissolved particles were surrounded by high densities of fine $Cr_{23}C_6$ precipitate, while in areas free from undissolved carbides, precipitates formed mainly on dislocations. The inhomogeneity of precipitation may originate from localized melting during the homogenization treatment. Within the grains there was sufficient solute supersaturation to cause repeated nucleation on climbing $a/2$ {1 1 0} dislocations; this occurred on {1 1 0} planes normal to the Burgers vector of the dislocation.

On ageing at 650° C matrix precipitate densities comparable to those in the Co–25.3 Cr–0.26 C alloy were produced in some areas, but the particle distribution was in general non-uniform.

3.5. Deformation substructures

Electron microscopical examination of samples of the Co–25.3 Cr–0.26 C alloy strained 1% in tension after solution treatment showed that deformation proceeded primarily by faulting. Although some undissociated dislocations were observed, intrinsic stacking faults were frequently seen to be grouped in clusters, and in some cases thin lamellae were formed (e.g. Fig. 5a) which produced additional spots in diffraction patterns. These spots could not usually be indexed according to f c c twinning, but could be indexed according to the h c p unit cell of the ϵ phase (Fig. 5b). This deformation-induced h c p phase possessed the characteristic f c c/h c p orientation relationship involving a parallelism between close-packed planes and directions. The streaking in the diffraction maxima in Fig. 5a results from the small dimension of the h c p lamellae along the streak direction [1 1 1]. The sharpness of the peaks in the streaked reflections indicates a high degree of order of the faults in the h c p stacking sequence, and thus demonstrates the presence of a lightly faulted h c p phase, rather than an f c c structure containing a high density of randomly distributed faults.

Larger strains (5 and 10%) induced by rolling this alloy at room temperature produced structures containing faulting on intersecting {1 1 1} planes and increased amounts of the h c p ϵ phase. Diffraction patterns frequently contained reflections from more than one variant of the h c p phase. The hardness of the solution-treated alloy (290 H_V) was markedly increased by deformation; strain of 1, 5 and 10% produced hardnesses of 305, 352 and 390 H_V respectively.

The Co–25 Cr–10 Ni–0.25 C alloys showed similar structural behaviour to that of the ternary alloys.

3.6. The effect of prior deformation on ageing

Samples of the Co–25.3 Cr–0.26 C alloy were aged at 650 and 700° C for times up to 500 and 100 h respectively after 1% and 10% deformation, to investigate the influence of the pre-existing dislocation substructure on the ageing behaviour.

3.6.1. 1% deformation

The modes of precipitation were not markedly changed by 1% prior deformation. Thus, the density of matrix precipitation was similar to that in specimens aged without deformation. Precipitation was also observed in association with extrinsic stacking faults, although the tendency was clearly for these to be produced near to the intrinsic deformation faults and in association with dislocations. A number of faulted loops were produced around matrix particles, being mainly in areas largely free from pre-existing dislocations. The dark-field micrograph of the structure after 24 h at 660° C (Fig. 6) allows the distinction to be made between the intrinsic deformation faults (I) and the extrinsic faults produced during ageing (E). Thus, extrinsic fault formation appears to be associated with intrinsic faulting. In some

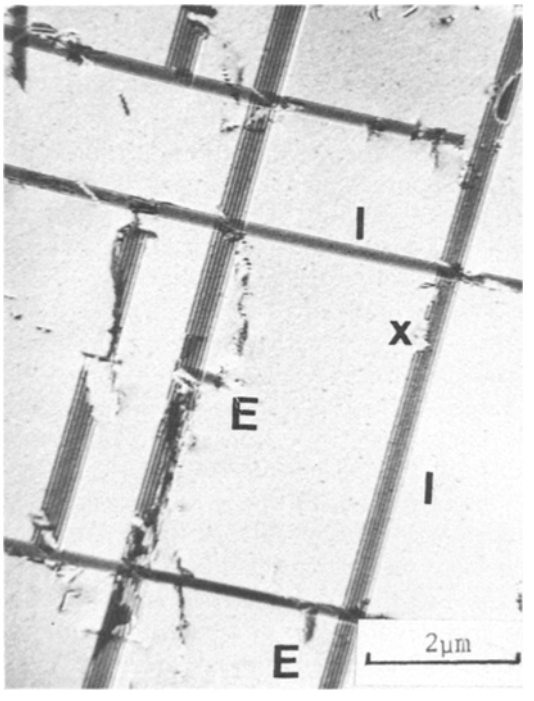

Figure 6 Co–25Cr–0.26C alloy solution treated 1 h at 1300° C, water quenched and deformed 1%; aged 24 h at 650° C Dark-field micrograph (g = 1 1 1) showing intrinsic (I) and extrinsic (E) faults. At X fringe contrast is absent due to formation of extrinsic fault on the same plane removing the intrinsic fault.

regions, the normal fringe contrast of the intrinsic faults is seen to be absent, e.g. at X, and this was shown to be due to the formation of an extrinsic fault on the same plane, which removes the intrinsic fault.

The overall rate of precipitation in the f c c matrix did not appear to be changed by 1% deformation. However, $Cr_{23}C_6$ precipitation in the form of plates or lath-shaped particles was observed within the thin lamellae of h c p ϵ phase, being nucleated at defects. The orientation relationship was found to be $(1\,1\,1)_{Cr_{23}C_6} \| (0\,0\,0\,1)_{hcp}$, $[1\,1\,0]_{Cr_{23}C_6} \| [1\,1\,\bar{2}\,0]_{hcp}$. The habit plane was $(0\,0\,0\,1)_{hpc}$ and the growth direction was $\langle 1\,1\,\bar{2}\,0\rangle$. The observed orientationship relationship is closely similar to that observed between $Cr_{23}C_6$ and the f c c matrix.

The hardness changes on ageing were not studied in detail, but ageing for 1 h at 800° C produced a hardness of 360 H_V compared with 340 H_V for underformed material similarly aged; this small difference probably reflects the effect of deformation on the solution-treated material.

3.6.2. 10% deformation

On ageing for 5 h at 700° C after 10% deformation, rapid precipitation producing coarse particles of $Cr_{23}C_6$ occurred in bands of ϵ phase (similar to the effect observed in the material deformed 1%), while precipitation in f c c γ took place much more slowly (Fig. 7a). There was a low density of matrix precipitates of somewhat non-uniform distribution. Precipitation also occurred in association with stacking faults in a few instances, but the density of faults produced during ageing was drastically reduced by comparison with the material aged without deformation. With increase in ageing time, both carbide coarsening and recrystallization occurred concurrently. Recrystallization was accompanied by the transformation of the matrix to h c p ϵ phase. Fig. 7b shows the coarse, non-uniform dispersion of carbides present after 100 h at 700° C; various carbide morphologies are seen – rod-like, roughly equiaxed and lamellar, the latter apparently having formed in association with the recrystallization reaction.

The progress of concurrent precipitation and recrystallization was also examined for ageing at 650° C. The density of $Cr_{23}C_6$ precipitates within the f c c and h c p phases was significantly greater than at 700° C. Particle growth continued in both matrix phases, until after 300 h partial recrystallization had occurred. After 500 h, recrystallization was essentially complete and a non-uniform dispersion of $Cr_{23}C_6$ particles existed in a relatively fault-free h c p matrix. Fig. 8 shows various carbide morphologies (predominantly lamellar).

It was not always possible to differentiate between precipitates formed in the f c c matrix prior to recrystallization and those found in association with the recrystallization reaction in the h c p phase.

During ageing at 700° C the as-deformed hardness of 390 H_V was increased to ~430 H_V after 1 h, with little subsequent change up to 100 h. At 650° C the hardness level after 500 h was 440 H_V.

4. Discussion

4.1. The solution-treated state

In the cobalt-rich alloys the f c c phase was retained at room temperature. However, it was found that lowering the carbon content to 0.10 wt % in the case of the ternary Co–Cr–C alloy raised the f c c → h c p transition temperature (i.e. M_s) thus allowing some h c p ϵ phase to form. Some observations on a Co–10 Cr–0.1 C alloy showed that

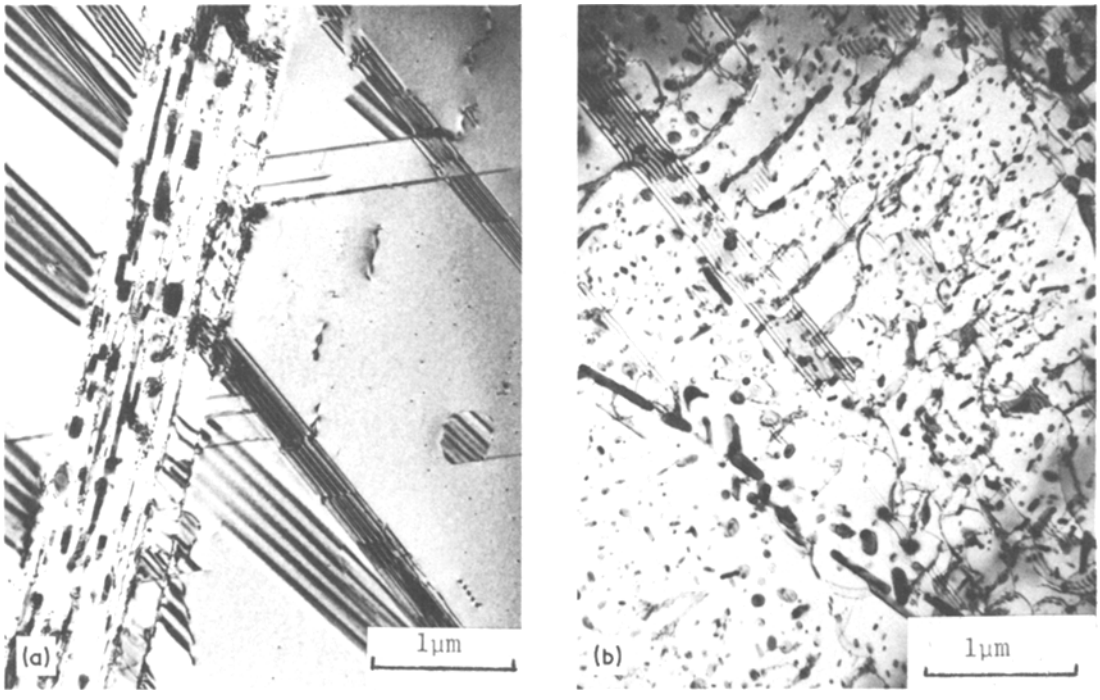

Figure 7 Co–25Cr–0.26C alloy solution treated 1 h at 1300° C water quenched and deformed 10%. (a) Aged 5 h at 700° C. Bright-field micrograph showing coarse precipitation in ϵ phase. (b) Aged 100 h at 700° C. Bright-field micrograph showing crystallization and carbide coarsening.

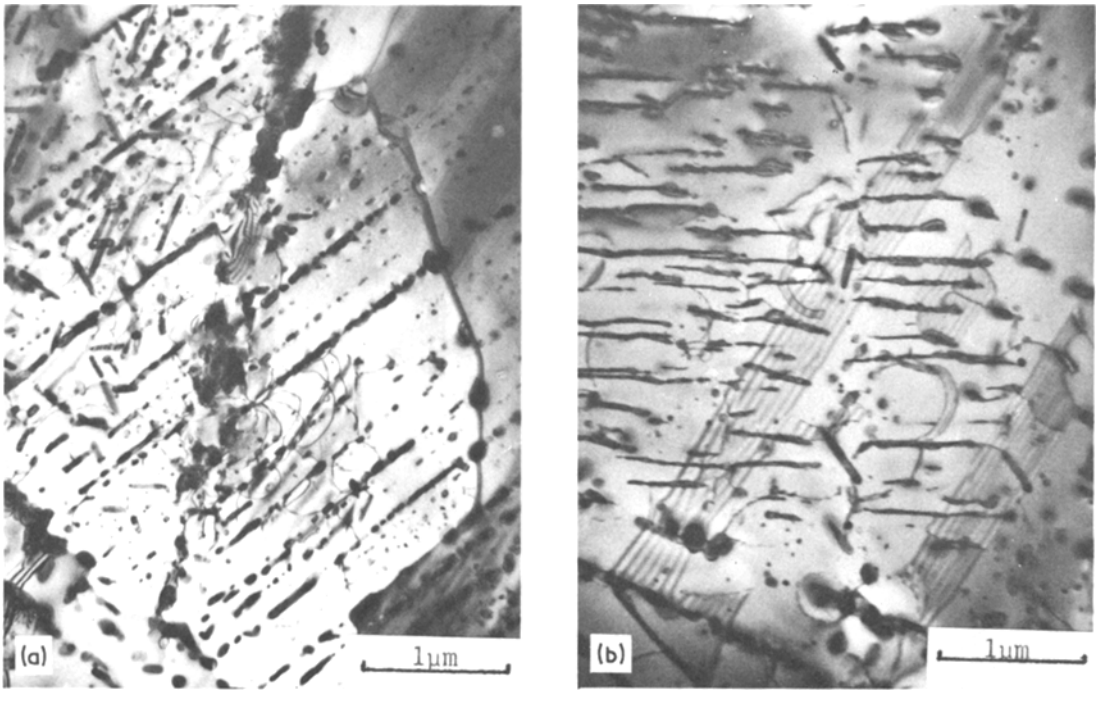

Figure 8 Co–25Cr–0.26C alloy solution treated 1 h at 1300° C, water quenched and deformed 10%; aged 500 h at 650° C. Bright-field micrographs (a) and (b) showing various carbide morphologies.

the f c c and h c p phases were heavily faulted and that the transformation therefore involves the motion of Shockley partial dislocations. In the Co–25.3 Cr–0.26 C alloy and the Co–25 Cr–10 Ni–C alloys, although the M_s was below room temperature, the formation of ϵ phase by deformation at room temperature indicated that M_d was above this temperature.

The observed dislocation structures in the present work conform to those expected on the basis of stacking fault energy. In the cobalt-based alloys the stacking fault energy was apparently so low that the dislocations were completely dissociated. Previous work [8] on the room temperature deformation of Co–Ni alloys indicated a transition from ϵ phase formation in the cobalt-rich range to deformation twinning (with uniformly distributed dislocations) as the nickel content is raised; the formation of dislocation "cell" structures was observed in the nickel-rich alloys. Co–Cr–Ni–C alloys studied in the present work showed the same trend with increasing nickel content. However it should be noted that chromium in the composition range used reduces the stacking fault energy [7]. In agreement with stacking fault energy data [9, 10] the presence of 20% cobalt in the Ni–Cr–Co alloy did not markedly influence the dislocation substructure, and in each of the nickel-rich alloys investigated, dislocations lay predominantly in planar arrays. In terms of Kotval's classification [1] the cobalt-rich alloys are considered to be class III (low SFE) and the nickel-rich alloys class II (medium SFE).

The density of faults in the cobalt-rich alloys as solution-treated was related mainly to the distribution and amount of undissolved carbides. Fault formation is attributed to the differential thermal contraction stresses between the carbide particles and the matrix, during quenching from 1300° C. In the nickel-based alloys, no dislocation dissociation was observed and the thermal stresses around the carbide particles were relieved by the punching-out of perfect dislocations.

4.2. Carbide precipitation

4.2.1. Matrix precipitation

Comparison of the Co–25 Cr–10 Ni–0.25 C alloy with the ternary Co–Cr–C alloy aged at 700° C shows a greater density of matrix precipitation in the former case, indicating a greater nucleation rate. The Co–25 Cr–10 Ni–0.15 C alloy showed an initial nucleation rate comparable to that in the Co–25.3 Cr–0.26 C alloy; therefore the effect of 10% nickel appears to be sufficient to outweigh any decrease in solute supersaturation with the lower carbon content. The predominant factor in this case may be an increase in the diffusion rate of the controlling species, brought about by the presence of 10% nickel. Other factors that may change with increase in nickel content of the Co–Cr–Ni–C alloys, and hence may affect the nucleation kinetics, are the equilibrium solubility of carbon in the matrix (and hence the supersaturation) and strain and surface energy parameters; however, data are lacking to show the extent to which these factors are significant.

Comparing the Ni–25 Cr–20 Co–0.15 C alloy with the Co–25 Cr–10 Ni–0.15 C alloy aged at 650° C (Fig. 4b) the density of matrix precipitates was somewhat lower in the nickel-based alloy. Furthermore, in this nickel-based alloy, precipitation was almost entirely heterogeneous at 700° C and only at 600° C was matrix precipitation the major decomposition mode. Thus, the results show that matrix precipitation in the nickel-rich alloys occurs less easily than in cobalt-rich alloys of similar carbon content.

The strong dependence of matrix particle density on ageing temperature in the Ni–Cr–Co–C alloy suggests a sharp change of supersaturation with temperature. The difference in precipitation characteristics between the cobalt-based and nickel-based alloys studied may be due partly to differences in carbon solubility and hence in carbon supersaturation, but differences in retained vacancy concentration may also be important [5].

The growth of the matrix-nucleated precipitates in the cobalt-based alloys and in the Ni–Cr–Co–C alloy, involving eventually the formation of a lath shape, was observed to occur in the manner described by Singhal and Martin [11]. The initial loss of coherency of matrix precipitate particles appears to occur by the formation of a single loop in both the cobalt-based and nickel-based alloys. In the Co–25.3 Cr–0.26 C alloy the loops were dissociated. However, in the nickel-based alloy the loops were perfect prismatic and lay on {1 1 0} planes of the matrix; this behaviour was noted to some extent in the Co–25 Cr–10 Ni–C alloys, which suggests that the type of loop formed is dependent on the stacking fault energy.

4.2.2. Dislocation-nucleated precipitation

In the cobalt-based alloys the main mode of hetero-

geneous nucleation was the repeated nucleation on Frank partial dislocations associated with stacking fault formation; the nucleation and growth processes, including the behaviour in regions adjoining grain boundaries, have been discussed elsewhere [5].

In the Co–25.3 Cr–0.26 C alloy deformed before ageing, nucleation occurred at defects within the lamellae of h c p ϵ phase. In the transformation of the f c c matrix to ϵ phase that accompanies recrystallization, the ϵ appears to form by a diffusional mode rather than by martensitic transformation of the solute-depleted f c c phase on subsequent cooling. This can be inferred from the fact that the recrystallized areas contained only a low density of stacking faults and dislocations, whereas a martensitic transformation on cooling would produce a heavily faulted h c p phase; however, the possibility may exist of a non-martensitic transformation during cooling producing an equiaxed h c p structure [12]. The lamellar carbides present after long ageing times probably formed in association with the movement of a boundary between recrystallized and unrecrystallized matrix regions, i.e. by a discontinuous precipitation reaction. Observations of carbide precipitation in the ϵ phase and of the simultaneous occurrence of recrystallization and carbide coarsening have been reported for Co–Cr–Mo–C alloys [6].

With increasing nickel content there was a trend to dislocation climb precipitation. $Cr_{23}C_6$ precipitate growth occurred more rapidly in the nickel-based alloy than in cobalt-based alloys of similar carbon content. At 700° C precipitation was almost completely dislocation-nucleated and it appears that the undissociated $a/2\langle 1\,1\,0\rangle$ dislocation is more effective as a nucleation site and as a source of solute by pipe diffusion, than is the Shockley partial dislocation in the cobalt alloys. The increased efficiency as a nucleation site is consistent with the larger value of the Burgers vector [13]. Extrapolation of available high temperature diffusion data indicates that at a typical ageing temperature of 700° C the rate of chromium diffusion in Ni–Cr alloys is ~4 times greater than in the comparable Co–Cr alloys. Assuming that chromium diffusion is rate controlling, this could significantly affect the precipitation kinetics.

Previous studies of carbide precipitation in association with climbing $a/2\langle 1\,1\,0\rangle$ dislocations have shown that climb may take place on $\{1\,1\,0\}$, $\{1\,0\,0\}$, or $\{1\,1\,1\}$ planes [14, 15]. The present results in the nickel-rich alloy demonstrate that the selection of climb plane can be influenced by particle shape effects. The formation of thin, lath-like particles of $Cr_{23}C_6$ in the Ni–25 Cr–20 Co–0.15 C alloy along $\langle 1\,1\,0\rangle$ directions not contained in the slip plane of the dislocation, forces dislocation climb to occur on $\{1\,1\,0\}$ and $\{1\,1\,1\}$ planes. This process is similar to that observed in a steel of composition 16 Cr–22 Ni–0.28 C by Kegg and Silcock [16] who showed that (i) when the lath axis is normal to the Burgers vector, climb occurs on the $\{1\,1\,0\}$ planes normal to the Burgers vector, (ii) when the lath is at 60° to the Burgers vector, climb occurs on a $\{1\,1\,1\}$ plane which contains the lath axis and is at 55° to the Burgers vector.

In the present case both of these configurations have been observed, with $\{1\,1\,0\}$ climb predominating, although frequently the irregular nature of the climb process made positive identification of the climb planes impossible. At lower ageing temperatures climb precipitation was initiated by loop formation at growing matrix particles in a similar manner to that in the cobalt alloys. In this case subsequent climb took place on $\{1\,1\,0\}$ planes since the Burgers vector was normal to the lath axis.

The climb process was fairly irregular so that meaningful quantitative data could not be obtained. However, examination of a number of precipitate arrays indicated that the number of vacancies produced by climb (determined from the area of climb) was easily sufficient to satisfy the requirements of the growing particles.

5. Conclusions

(1) The addition of 10 wt % nickel to a Co–25 Cr–0.26 C alloy increased both the rate of nucleation and growth of matrix-nucleated $Cr_{23}C_6$ particles; the incubation time for stacking fault precipitation is reduced, and the number of extrinsic faults generated is increased.

(2) In an alloy containing Ni–25 Cr–20 Co–0.15 C there is little matrix precipitation and carbide nucleation occurs predominantly on dislocations in lath-shaped form. The stacking fault energy appears to affect the relative rates of heterogeneous and "homogeneous" nucleation by influencing the nature and distribution of dislocations in the as-quenched state and hence, indirectly, the retained vacancy concentration.

Repeated nucleation of $Cr_{23}C_6$ occurs solely in association with climbing dislocations and there is no evidence for Frank partial precipitation; the climb plane may be {1 1 0} or {1 1 1}.

(3) The transition from "stacking fault precipitation" (Frank partial precipitation) to dislocation climb precipitation as the nickel content is increased cannot be uniquely ascribed to a single factor. Relevant factors include increase in stacking fault energy, the ease of nucleation and the rate of precipitation. Also the degree of supersaturation after solution treatment may be lower in the nickel-rich alloys than in the cobalt-rich alloys.

(4) Substantial hardening can be achieved from carbide precipitation, particularly in the cobalt-rich alloys containing 0.25% C. The precipitate dispersions are more stable in the cobalt-rich alloys, with less rapid over-ageing than in the nickel-rich alloys.

(5) Deformation of the Co–25 Cr–0.26 C alloy produced faulting and h c p ϵ phase. During ageing after deformation, carbide precipitation occurred in both the h c p and f c c phases; on prolonged ageing after 10% deformation, carbide particle coarsening occurred together with the f c c $\rightarrow$ h c p transformation of the matrix, in association with recrystallization.

Acknowledgements

The authors wish to acknowledge the provision of research facilities by Professor J. G. Ball and the supply of the alloy by CNRM by arrangement with Mr. J. Williams of the Cobalt Research Centre. One of the authors (PAB) acknowledges the award of an SRC studentship. The work formed part of a thesis submitted by one of the authors (PAB) for the Ph.D. degree of London University.

References

1. P. S. KOTVAL, *Trans. AIME* **242** (1968) 1651.
2. C. P. SULLIVAN, M. J. DONACHIE Jr and F. R. MORRAL, "Cobalt-base superalloys", (Centre D'Information du Cobalt, Brussels, 1970).
3. V. RAMASWAMY, P. R. SWANN and D. R. F. WEST, Proceedings Fifth International Materials Symposium, Berkeley, California (John Wiley, New York, 1972) p. 637.
4. *Idem,* Third International Conference on the Strength of Metals and Alloys (Institute of Metals and Iron and Steel Institute, London, 1974) p. 69.
5. P. A. BEAVEN, P. R. SWANN and D. R. F. WEST, *J. Mater. Sci.* (in press).
6. J. B. VANDER SANDE Jr, J. R. COKE and J. WULFF, *Met. Trans. AIME* **7A** (1976) 389.
7. J. H. DAVIDSON, Seven Springs Conference on Superalloys (Claitors Publishing Division, 1977) p. 275.
8. A. KORBAL and S. GORCZYCA, *Phys. Met. Metall.* **31** (1971) 163.
9. E. KOSTER, A. R. THOLEN and A. HOWIE, *Phil. Mag.* **10** (1964) 1093.
10. B. BEESTON and L. FRANCE, *J. Inst. Metals* **96** (1968) 105.
11. L. K. SINGHAL and J. W. MARTIN, *Acta Met.* **16** (1968) 1159.
12. A. GIAMEI, J. BURMA and E. J. FREISE, *Cobalt* **39** (1968) 88.
13. J. W. CAHN, *Acta Met.* **5** (1957) 169.
14. M. C. CHATURVEDI, R. W. K. HONEYCOMBE and D. H. WARRINGTON, *J. Iron Steel Inst.* **206** (1968) 1236.
15. J. M. SILCOCK and A. W. DENHAM, "The Mechanism of Phase Transformations in Crystalline Solids" (Institute of Metals, 1968) p.59.
16. G. R. KEGG and J. R. SILCOCK, *Scripta Met.* **8** (1974) 1245.

Received 14 March and accepted 3 May 1978.